Fire Safety Journal 116 (2020) 103186

Contents lists available at ScienceDirect

Fire Safety Journal

journal homepage: http://www.elsevier.com/locate/firesaf

Mesoscale numerical modeling and characterization of the effect of reinforcement textile on the elevated temperature and tensile behaviour of carbon textile-reinforced concrete composite

Manh Tien Tran [a], Xuan Hong Vu [b,*], Emmanuel Ferrier [b]

[a] Hanoi University of Mining and Geology (HUMG), No18, Pho Vien Street, Duc Thang Ward, Bac Tu Liem District, Ha Noi City, Viet Nam
[b] Université de LYON, Université Claude Bernard LYON 1, Laboratoire des Matériaux Composites pour la Construction LMC2, France

ARTICLE INFO

Keywords:
Textile-reinforced concrete (TRC)
Carbon textile
Refractory concrete
Elevated temperature
Mesoscale modeling

ABSTRACT

This paper presents both experimental and mesoscale modeling results of the direct tensile behaviour of two carbon TRC composites at elevated temperatures ranging from 25 °C to 600 °C. Two reinforcement carbon textiles were manufactured industrially in the factory with different geometries and treatment products to improve the textile/matrix bond. For the numerical approach, the input data of the numerical models were chosen from the experimental results of TRC component materials (carbon textiles, cementitious matrix). The carbon TRCs gave the strain-hardening behaviour with different phases depending on elevated temperature levels. Furthermore, the numerical model highlighted the failure mode with the transversal cracks on the specimen surface, using the crack damage model for the concrete matrix. The effect of elevated temperature on the TRC behaviour and performance of the TRC was determined and analyzed by comparing it with the results obtained at room temperature. By comparing the experimental results on both carbon TRCs, the effect of the reinforcement textile on the thermomechanical behaviour of TRC composites could also be highlighted and discussed. The numerical results of the carbon TRCs at elevated temperature levels were also compared with experimental results. The good agreement obtained between the experimental and numerical results demonstrated the rationality of this numerical model.

1. Introduction

Over recent decades, textile-reinforced concrete composites (TRC) have been increasingly applied in the civil engineering field. They have usually been used to strengthen or reinforce the structural elements of old construction works (buildings, tunnels, etc) or serve as constituent elements of new structures [1–4]. In these cases, the performance of TRC composites plays an important role in the loading capacity of structures. The mechanical behaviour of TRC composites at room temperature has been characterized experimentally by tensile and flexural tests in the literature [4–7]. Three phases of hardening behaviour have been distinguished, which are highly dependent on the characteristics belonging to the reinforcement textile, such as the fiber type, textile geometry, and textile treatment products [5,8–10]. However, this behaviour is less well determined in certain specific conditions such as the corrosion environment, durability and elevated temperature.

Previous experimental studies [11–14] showed that when concretes, with or without reinforcement by various discontinuous fibers within their cementitious matrices, were subjected to elevated temperatures, their physical and/or mechanical properties gradually evolved with increasing temperature. Previous experimental results also indicated that concrete residual compressive strength decreases with increasing temperature [13,14] and the decrease in the residual compressive strength of ordinary concrete was greater than that in high-performance concrete [14]. Previous studies related to the effects of various discontinuous fibers, added in the matrix of concretes, such as polypropylene fibres [11], steel fibers and polypropylene fibers [12], highlighted that the addition of steel fibres and polypropylene fibers effectively improved the residual compressive and flexural properties of concretes at high temperatures. When concretes were reinforced by various continuous fibers (or continuous reinforcement textiles) within their cementitious matrices and then subjected to elevated temperatures, their tensile properties (like ultimate strength, ultimate strain, stiffness) at elevated temperatures were significantly improved [10,15,16]. The

* Corresponding author.
E-mail addresses: tranmanhtien@humg.edu.vn (M.T. Tran), Xuan-Hong.Vu@univ-lyon1.fr (X.H. Vu), emmanuel.ferrier@univ-lyon1.fr (E. Ferrier).

https://doi.org/10.1016/j.firesaf.2020.103186
Received 24 December 2019; Received in revised form 30 June 2020; Accepted 4 July 2020
Available online 3 August 2020

results showed that the improvement of TRC resistance greatly depended on the strength of continuous textile reinforcement [10,15,16]. Furthermore, for the textile/matrix bond, this factor also greatly depends on the thermal physical and chemical response of the treatment product used for the reinforcement textile in the manufacturing procedure to improve its bond strength [15,17–19]. The effect of textile treatment on the thermomechanical behaviour and failure modes of carbon textile was highlighted and analyzed in Ref. [20,21]. The following paragraphs present the previous research (experimental and numerical) which focused on the mechanical behaviour of TRC composites at different temperatures. The objective of this study is presented at the end of the introduction of this paper.

1.1. Tensile behaviour of TRC composites at different temperatures

Until now, there have been very few studies on the behaviour of TRC composites under mechanical loading and elevated temperature loadings due to test set-up difficulties. The literature includes fire tests performed on high-performance concrete thin-plates, reinforced with basalt fibre-reinforced polymer mesh [22], and on I-shaped beams reinforced with glass-fibre and carbon-fibre mesh grids [23]. Also, few studies have been performed on textile-reinforced mortar (TRM) in comparison with fibre reinforced polymer (FRP) used as strengthening materials of structure specimens at high temperatures [24–26]. They were conducted to characterize the elevated temperature behaviour under shear and flexural stress of structures strengthened by TRM or FRP [24–26]. All these tests [22–26] aimed to identify fire or elevated temperature resistance under different load types of TRC at the structure scale.

Furthermore, few studies have been performed on TRC specimens to characterize the residual behaviour under tension of TRC composites after exposure to elevated temperatures (called residual condition) [15,18,19,27–29]. All the experimental results obtained showed a strain – hardening behaviour of TRC composites with different numbers of phases, depending on the preheating temperature levels imposed. The positive effect of preheating loading at a temperature level ranging from 75 °C to 200 °C on the residual behaviour of TRC composites was highlighted in previous studies [15,18,19,27–29]. This result was due to the positive effect of the melting – curing process of the textile treatment product, which significantly improved the mechanical properties of the reinforcement textiles used, as well as the bond strength between the textile and the matrix interface. However, after exposure to temperatures higher than 400 °C, the TRC composites presented a significant decrease in residual strength because of the oxidation of the fibres during preheating.

Up to now only a small number of studies have been conducted on the tensile behaviour of TRC composites under simultaneous mechanical loading and elevated temperatures [28,30–34]. Ehlig et al. [32] studied the influence of the rate of temperature increase on the rupture temperature of carbon TRC specimens under a thermomechanical regime at a constant force. The effect of discontinuous short glass fibres on the thermomechanical behaviour of a glass TRC composite at elevated temperatures was investigated in Ref. [30]. Saidi et al. [34] studied the effect of water content in TRC on its behaviour at temperatures ranging from 75 °C to 800 °C. All the results found in the literature showed that the variable behaviour of TRC composites depends on several factors belonging to the reinforcement textile (reinforcement ratio, textile geometry, type of fiber and fiber treatment) or the cementitious matrix (type of matrix, matrix water content, modification of the matrix at different temperatures).

To take into account all the factors mentioned above with a single experimental approach is not feasible due to issues of time and cost. Therefore, the numerical approach is a reasonable choice for studying the effect of factors on the elevated temperature behaviour of TRC composites. The global behaviour of TRC material at elevated temperatures can be predicted using a mesoscale numerical model with the input data of the constitutive materials (reinforcement textile, cementitious matrix, and textile/matrix interface).

1.2. Mesoscale numerical studies of TRC behaviour

Several numerical studies were performed to characterize the global behaviour in tension or flexion of TRCs at room temperature from the input data of the constituent materials [35–40]. These mesoscale models presented reasonable results in comparison with those of the experiment. However, at elevated temperature, only a small number of numerical studies have been performed at the mesoscale on the elevated temperature behaviour of TRC composites [18,41]. Blom and Wastiels [41] developed an analytical model based on the ACK theory (proposed by Aveston, Cooper and Kelly) using the method of Soranakom and Mobasher [6] to predict elevated temperature behaviour from experimental data. Rambo et al. [18] used a finite-difference model, by taking into account the non-linear spring model for the textile/matrix interface and a brittle model with no strain-softening response for the cementitious matrix, to simulate the tensile behaviour of the basalt TRC composite. These numerical results showed the “stress-strain” relationships at different temperatures as well as the effect of the interface model on the third phase of composite behaviour, and thus the spacing of cracks. These numerical studies showed *a* good agreement with experimental results.

All the numerical studies mentioned above [6,18,35–41] were based on different calculation methods (finite element method, different finite method, and analytical method), and they have contributed significantly to knowledge relating to the mesoscale modeling of TRC behaviour at different temperatures. However, certain of the scientific details of these models required improvement. Firstly, there was the material model used for the cementitious matrix in the numerical calculation. Nonlinear behaviour was generally proposed for the cementitious matrix in the TRC composite, although, in reality, the mechanical behaviour of the cementitious matrix is very complex due to the multi-cracks that can influence the global behaviour of the TRC composite [9]. Secondly, there was the “bond-slip” model for the textile/matrix interface in the TRC composite. The bilinear model was successfully used for the textile/matrix interface in several numerical studies [35,41,42]. However, it could be considered to have a perfect connection between the textile and the matrix if there was no slip at the textile/matrix interface during the test. In the paper of Larrinaga et al. [39], the finite element (EF) model for the tensile behaviour of a textile reinforced mortar (TRM) composite revealed no significant dependence on the basalt textile-mortar interface. This numerical model gave results in agreement with those of the ACK model and experiment. Thus, the textile/matrix interface behaviour could be (or not be) taken into account, depending on the failure mode of TRC specimens at elevated temperature. If the TRC specimen fails under tension through the rupture of its textile reinforcement with surface multi-cracking, the adhesion between the textile and the matrix could be considered that as perfect.

1.3. Objective of this study

To the best of the authors’ knowledge, no results are available concerning the effect of carbon textiles (textile geometry and treatment) on the thermomechanical behaviour of carbon TRC composites at elevated temperatures. There are also no numerical results regarding mesoscale modeling using the finite element method for the elevated temperature behaviour of TRCs. Thus, the aim of this study is to contribute to knowledge of the effect of carbon textile (textile geometry and treatment) on the elevated temperature behaviour of TRC composites, using both experimental and numerical approaches. In this paper, two reinforcement carbon textiles were used to reinforce the refractory matrix for a fire application. These textiles were manufactured industrially in the factory with different geometries and treatment products (epoxy resin and amorphous silica products) to improve the textile/matrix bond. The specimens of the two carbon TRCs studied were tested in

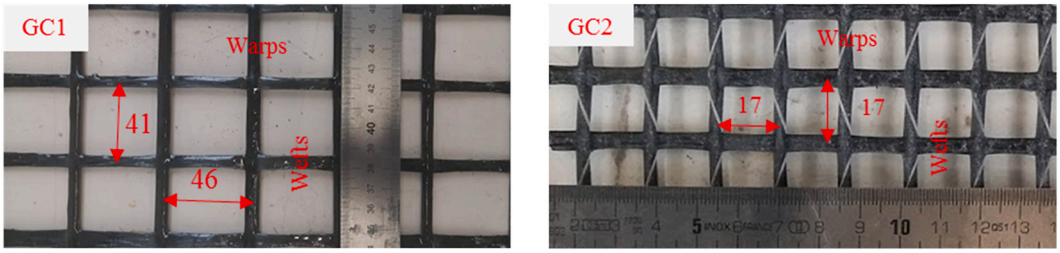

Fig. 1. Images of carbon textiles used in this experimental study.

Table 1
Results of the direct tensile tests performed on the carbon textiles and cementitious matrix [20,31].

Temperature (°C)	GC1 textile		GC2 textile		Cementitious matrix	
	Ultimate stress (MPa)	Young's modulus (GPa)	Ultimate stress (MPa)	Young's modulus (GPa)	Ultimate stress (MPa)	Young's modulus (GPa)
25	2616.6	256.2	1311.5	143.8	5.29	8.41
75	–	–	–	–	3.76	6.58
200	2169.5	201.6	1152.5	138.6	3.69	4.39
400	1652.2	138.8	708.8	107.1	3.28	3.09
500	795.7	77.6	308.1	39.7	2.90	2.29
600	204.9	29.5	–	–	2.54	1.67

thermomechanical regime at different temperature levels ranging from 25 °C to 600 °C. The effect of carbon textiles on the elevated temperature behaviour of TRC composites was highlighted and analyzed using experimental results. For the numerical approach, the input data were chosen from the experimental results of the TRC's component materials (carbon textiles, refractory matrix). These models can take into account the material damage for the cementitious matrix by including the cracking model. The numerical results will be compared and discussed in this paper to find agreement with the experiment.

2. Experimental works

This section presents the experimental approach followed in this study, including the composite materials used, the test procedure and the summary of tests.

2.1. Carbon TRC composites

The carbon TRC composites used in this experimental study were based on a refractory matrix and reinforced by carbon textiles. The component materials used (carbon textiles and cementitious matrix), as well as the preparation procedure of the TRC specimens, are presented in the following paragraphs.

2.1.1. Carbon textiles

The continuous carbon textiles used (called GC1 and GC2 carbon textiles) in this experiment are commercial products manufactured industrially in grid form for application in civil engineering works. These textiles were treated with two different products as a coating: an epoxy resin product (completely pre-impregnated in epoxy resin) for the GC1 textile and another coating product with amorphous silica for the GC2 textile. The geometry of the textile grid in the longitudinal and transverse directions is 46 mm × 41 mm and 17 mm × 17 mm, respectively for carbon textiles GC1 and GC2 (see Fig. 1). The cross-section of the textile yarns (both warp and weft) is similar for both carbon textiles, 1.85 mm^2 for GC1 and 1.795 mm^2 for GC2. These carbon textiles were tested in thermomechanical conditions at different temperature levels ranging from 25 °C to 600 °C, as presented in Ref. [20]. Table 2 below presents the thermomechanical properties of both carbon textiles (GC1, GC2) such as ultimate stress and Young's modulus at elevated temperature levels.

2.1.2. Cementitious matrix

The cementitious matrix used in this experimental study was designed in laboratory conditions to produce carbon TRC specimens as in Ref. [31]. This matrix was based on calcium aluminate cement (CAC) with a calcium aluminate content of about 50%, and synthetic aggregates obtained by melting with an alumina content of about 40%. The high aluminate content of this matrix gives it good mechanical performance at elevated temperatures. The compressive strength of the cementitious matrix after 28 days at 25 °C is 58.1 MPa while its tensile mechanical properties were characterized in Ref. [31] from thermomechanical tests at different temperatures, as presented in Table 1.

2.1.3. Preparation procedure of TRC specimens

All the carbon TRC specimens (called F.GC1 and F.GC2 in this study) were prepared in laboratory condition by using a hand lay-up method technique with the three following steps (see Fig. 2). Firstly, a rectangular wooden mold of dimensions 740 mm × 500 mm (length x width) was prepared in which the carbon textiles were cut to size and tensioned by clamping mechanisms at two ends of the mold for one day to flatten the carbon meshes (see Fig. 2a). Afterwards, the hand lay-up molding technique was used to manufacture the TRC plates, as presented in Fig. 2b, one layer of matrix, then carbon textile layers and, finally, one other matrix layer. It was necessary to ensure that the reinforcement textiles were in the middle of the TRC plate thickness to guarantee the symmetry of the TRC composite specimens. Finally, these TRC plates were preserved in laboratory conditions for specimen curing (see Fig. 2c). After 28 days, the rectangular plates were cut to obtain the TRC specimens with different dimensions for both TRC composites, depending on the geometry of the carbon textiles (see Fig. 2d). The cross-sectional area of the TRC specimens was determined by the average of three measurements (width and thickness) at three different points of each sample. The reinforcement ratio was calculated as the ratio between the cross-section of the textile warps and that of the TRC composites (see Table 3).

2.2. Test setup

The thermomechanical tests were carried out on TRC specimens with the equipment used in the LMC2 laboratory (France), including: the control system (see Fig. 3a) and the experimental devices (see Fig. 3b). The experimental devices can apply tensile loading and elevated temperature simultaneously to TRC specimens. The imposed displacement

Table 2
List of tests carried out on the carbon TRC composite specimens; (*) only two tests were carried out at a temperature of 600 °C.

Designation of the specimens	Specimen dimensions [cross section, S(mm^2); length, l (mm)]	Reinforcement ratio (%)	Temperature (°C)	Exposure duration	Number of tests
F.GC1-T-1,2,3	11 × 65 (mm^2); 740(mm)	0.52	25, 75, 200, 400, 500, 600(*)	1h	17
F.GC2-T-1,2,3	11.5 × 51 (mm^2) 740(mm)	0.92	25, 75, 200, 400, 500, 600(*)	1h	17
Total of tests					34

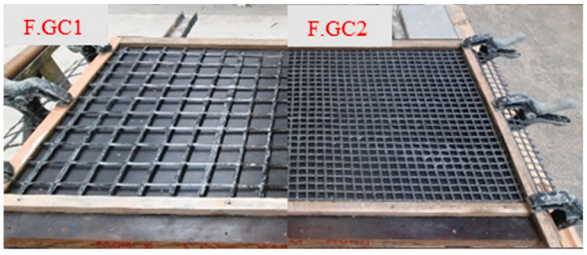

(a) Molding preparation and flattening for carbon textiles (the first step).

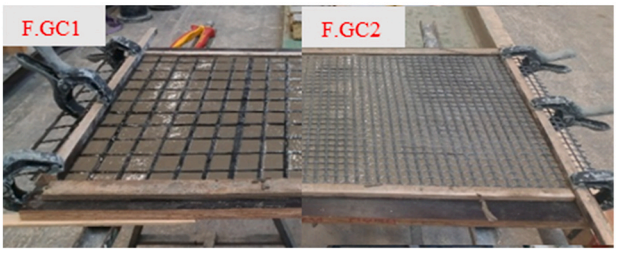

(b) Hand lay-up molding (the second step).

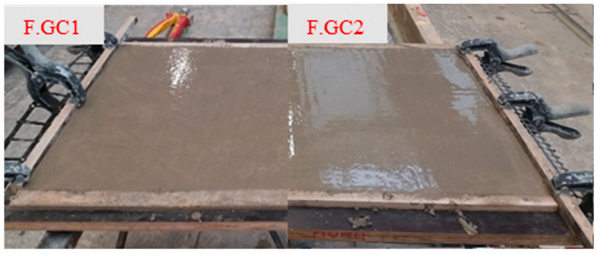

(c) Preserving TRC plates in laboratory conditions (the final step).

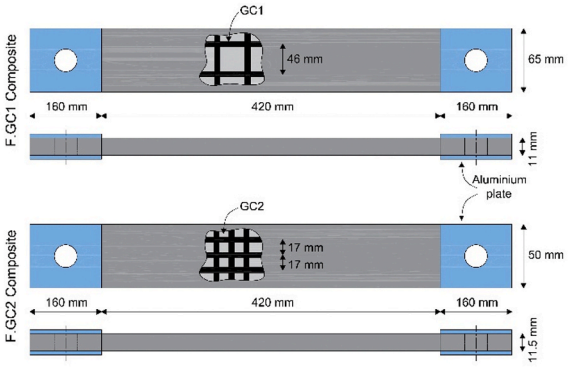

(d) Dimensions of both TRC specimens.

Fig. 2. Preparation procedure of rectangular composite plates (a,b,c) and dimensions of carbon TRC specimens (d).

Table 3
Thermomechanical properties (average values) of both carbon TRC composites; (the standard deviation value for each parameter is presented in parallel).

T (°C)	F.GC1					F.GC2				
	First crack values		Post crack values			First crack values		Post crack values		
	$\sigma_{T,I}$ (MPa)	$E_{T,I}$ (GPa)	$\sigma_{T,UTS}$ (MPa)	$\varepsilon_{T,UTS}$ (%)	$E_{T,III}$ (GPa)	$\sigma_{T,I}$ (MPa)	$E_{T,I}$ (GPa)	$\sigma_{T,UTS}$ (MPa)	$\varepsilon_{T,UTS}$ (%)	$E_{T,III}$ (GPa)
25	4.25 (0.48)	10.57 (1.46)	12.76 (0.48)	0.866 (0.066)	3.04 (0.25)	6.38 (0.54)	11.33 (0.63)	10.30 (0.41)	0.813 (0.071)	2.50 (0.43)
75	2.25 (0.15)	5.86 (1.05)	12.17 (0.73)	1.084 (0.118)	1.18 (0.06)	4.71 (0.78)	9.03 (1.08)	9.64 (0.11)	0.694 (0.128)	1.76 (0.26)
200	2.12 (0.16)<	4.98 (0.46)	11.00 (0.96)	0.906 (0.134)	1.09 (0.15)	3.79 (0.37)	8.48 (0.37)	6.95 (0.35)	0.497 (0.059)	2.13 (0.08)
400	2.36 (0.58)	5.59 (0.58)	7.06 (0.40)	1.117 (0.198)	0.60 (0.06)	3.63 (0.53)	7.13 (0.73)	6.11 (0.41)	0.359 (0.045)	1.15 (0.30)
500	2.20 (0.61)	3.15 (0.48)	4.63 (1.02)	0.829 (0.098)	0.59 (0.10)	3.39 (0.43)	3.75 (0.34)			
600	1.83 (0.30)	2.77 (0.43)				2.40 (0.39)	2.14 (0.02)			

of the traverse of the machine and the elevated temperature loading were controlled by the control system while the laser sensor was activated to measure the deformation of a central part of the TRC specimen placed inside the furnace during an elevated temperature thermomechanical test. The gauge length between the laser sensor points was about 10 cm. For the temperature measurement, three thermocouples were attached to the surface of the TRC specimen at points equidistant from the middle of the furnace, as presented in Fig. 3b. The loading path of the thermomechanical tests with three phases, presented in Fig. 3c, was controlled by the control program of Test-Expert II software. This test setup has been used to characterize the elevated temperature behaviour of various composite materials such as Textile reinforced concrete (TRC), Carbon Fiber Reinforced Polymer (CFRP) and carbon textile, etc., in previous studies by the author's team [20,28,31,43,44].

2.3. Summary of tests

Table 2 shows the list of specimens for the thermomechanical tests in this experiment. For each temperature level, three tests were carried out to ensure the convergence of the experimental results, except at a

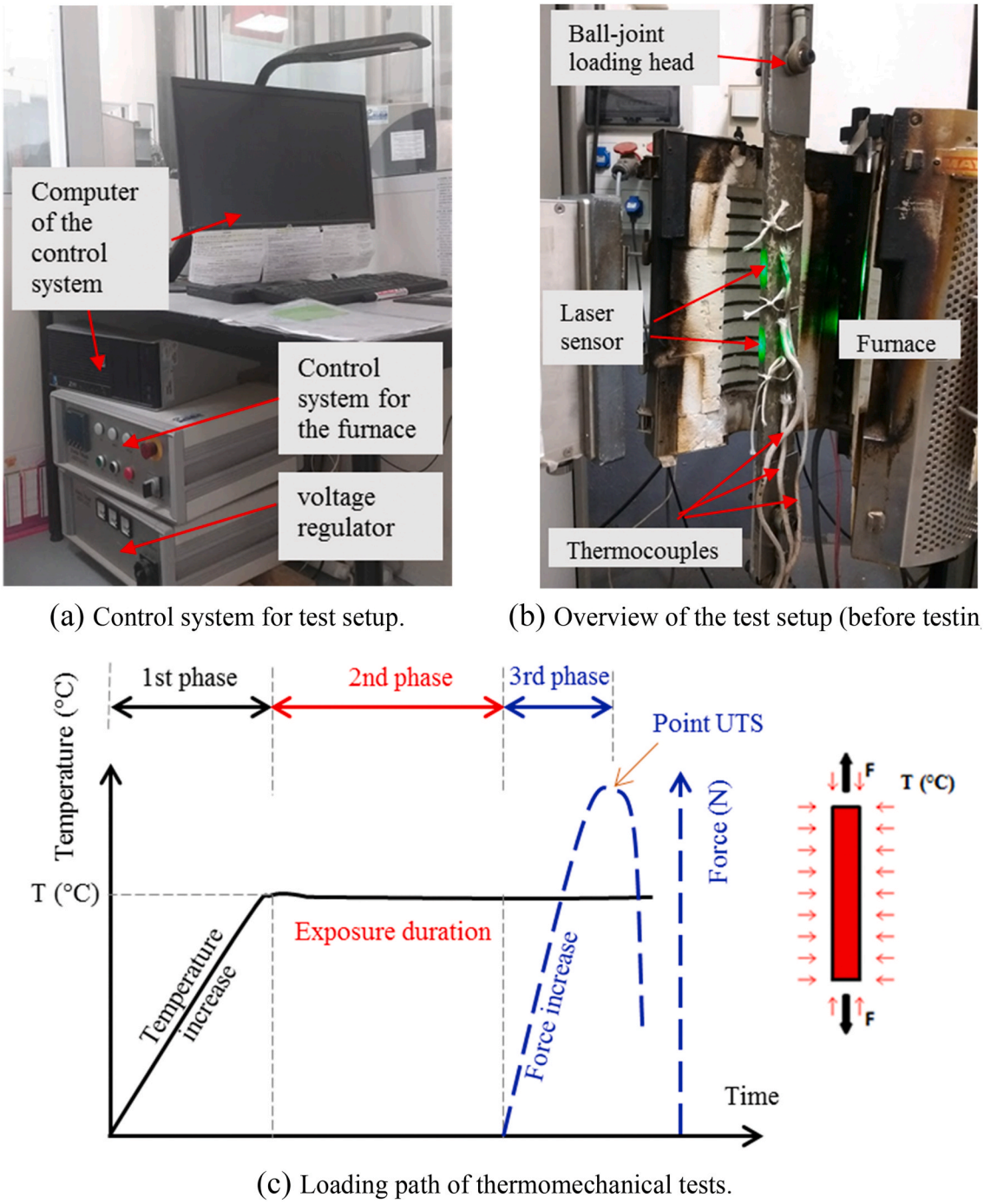

Fig. 3. Thermomechanical test setup and loading path in the experiment.

temperature level of 600 °C, for which only two thermomechanical tests were performed. Thus, there were 34 tests in this experiment for both carbon TRCs at different temperatures ranging from 25 °C to 600 °C.

3. Results and discussion

3.1. Experimental results

This section presents the results of the thermomechanical tensile tests performed on the specimens of both the carbon TRCs studied, including on thermomechanical behaviour, the evolution of thermomechanical properties as a function of increasing temperature, and the failure mode of the TRC composites.

3.1.1. Strain hardening behaviour of carbon TRC composites

Fig. 4 shows "axial stress – axial thermomechanical strain" curves for both TRC composites (F.GC1 and F.GC2) under temperature levels ranging from 25 °C to 600 °C. In this figure, one average "axial stress – axial thermomechanical strain" curve is represented for three thermomechanical tests carried out on the carbon TRC specimens for each temperature level. It was found that the carbon TRC specimens presented strain hardening behaviour at low-temperature levels and brittle behaviour at high-temperature levels. The change of their thermomechanical behaviour with increasing temperature depended on the effect of elevated temperature on the reinforcement textile. This effect was also the main cause leading to the reduction of the ultimate strength of the specimens of both carbon TRC composites studied as a function of

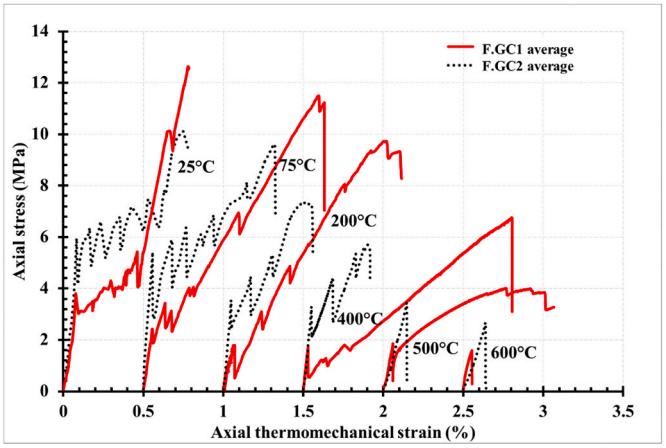

Fig. 4. Thermomechanical behaviour of the specimens of the two carbon TRCs studied (F.GC1 and F.GC2) at different temperature levels.

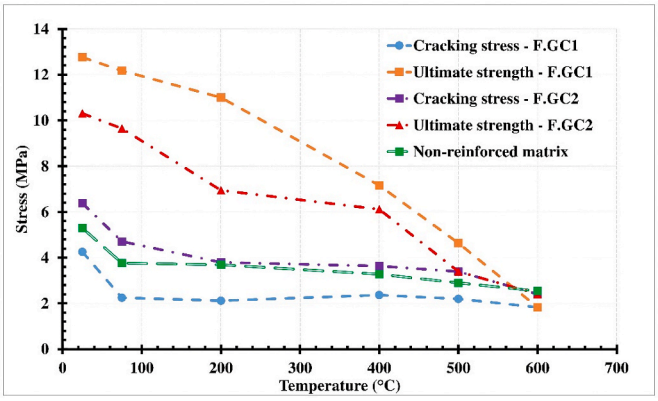

Fig. 5. Evolution of cracking stress and ultimate strength of the two carbon TRCs studied (F.GC1 and F.GC2) as a function of temperature.

increasing temperature. Fig. 4, clearly shows the cracking phase in the case of composite F.GC2 at temperature levels ranging from 25 °C to 400 °C by the drops in axial stress whereas this phase for the specimen F. GC1 is not clear at the temperature below 200 °C. The drops in the axial stress of the "axial stress – axial thermomechanical strain" curve correspond to the cracks on the surface of the carbon TRC specimens. Regarding the evolution of the cracking stress, it was found that its value decreased gradually with the increase of elevated temperature. However, this evolution occurred at two different levels for both the carbon TRCs studied although they were based on the same cementitious matrix.

To characterize the thermomechanical behaviour and identify the properties of the carbon TRCs studied, an idealization of the "axial stress-axial strain" curve and notations was used. The properties of the TRC specimens were defined as presented in previous research by the authors [31]. The crack stress $\sigma_{T,I}$ was defined by the average stress in the TRC composite at the beginning of cracking while the initial rigidity $E_{T,I}$ was the stiffness of the composite before macro-cracking (defined as the average slope of the first phase of the "stress-strain" curve. The post-cracked rigidity $E_{T,III}$ was defined as the average slope of the thirst phase of the "stress-strain" curve, because after the complete cracking of the cementitious matrix, there was a stiffer response from the carbon TRC and the increase of the applied axial displacement generated a nearly linear increase of stress. The ultimate strength $\sigma_{T,UTS}$ was defined as stress at the point corresponding to the rupture of the specimen. These main thermomechanical properties of the two carbon TRCs studied are presented in Table 3 below.

3.1.2. Evolution of thermomechanical properties as a function of elevated temperature

Fig. 5 shows the evolution of the cracking stress and ultimate strength of the two carbon TRCs studied as a function of elevated temperature in comparison with that of the non-reinforced matrix specimens in Ref. [31]. As the results show, the ultimate strength of F.GC1 specimens fell according to a long curve from 12.76 MPa at room temperature to 1.83 MPa at 600 °C while the ultimate strength evolution of the F.GC2 specimens can be divided into two intervals of temperature: from 25 °C to 400 °C and from 400 °C to 600 °C. This result is in good agreement with the observation of the experimental results performed on the carbon textile specimens (GC1 and GC2) [20]. Regarding the evolution of cracking stress with elevated temperature, a similar reduction was observed for the specimens of the two carbon TRCs studied with that of the non-reinforced matrix specimen, but on two different levels depending on the reinforcement textile: a higher level for F.GC2 and a lower level for F.GC1. The effect of reinforcement textile on cracking stress is discussed again in section 3.2.

3.1.3. Failure modes

Fig. 6 shows the specimens of the two carbon TRCs studied after the thermomechanical tests at different temperature levels ranging from 25 °C to 600 °C. All the specimens of the carbon TRC composites studied presented a fragile failure mode with cracks on the surface of the specimens and finally abrupt breaking. This failure mode was also identified by a significant drop in axial stress on the axial stress-axial strain curve of their thermomechanical behaviour. At elevated temperatures above 500 °C, it could be observed that the mono-filaments of carbon textiles remained connected with each other at the broken section because of the elevated temperature loading.

As can be seen with the failure modes presented in Fig. 6, the number of cracks decreased with increasing temperature for both carbon TRC specimens. At low-temperature, the bond strength of the carbon textile/matrix interface remained strong enough to allow the force transfer from the reinforcement textile to the cementitious matrix. At the limit state, cracking occurred in the cementitious matrix at the weakest cross-section (or the most dangerous cross-section). This process of the next cracks occurring depended on a parameter called load transfer length (δ_0), in line with [47]. With the load transfer length in the vicinity of a crack, the cementitious matrix strain decreases until it becomes nil at the crack location. Thus, the cracking space depends on load transfer length. At a temperature higher than 200 °C, the bond strength of the textile/matrix interface decreased due to the elevated temperature effect. This was the mechanism that prevented multi-cracking from developing on the surface of the TRC specimens.

3.2. Discussion

This section presents the discussion concerning the effect of carbon textiles on the elevated temperature behaviour and mechanical properties of TRC composites.

3.2.1. Effect of carbon textile on the ultimate strength of TRC composites

Figs. 4 and 5 show the effect of carbon textiles on the ultimate strength of TRC composites. The F.GC1 composite specimens gave higher values in ultimate strength at the same temperature levels although their reinforcement ratio was smaller, about half that of the F. GC2 specimens (0.52% for F.GC1 and 0.92% for F.GC2). This result was due to the effect of the textile treatment on the ultimate strength of the textile yarn. The treatment with the epoxy resin product ensured the interaction of the mono-filaments inside the textile yarn of the GC1 carbon textile. Thus, the longitudinal yarn (the warp) of the GC1 carbon textile's capacity in strength was twice as high as that of textile GC2 [20]. Furthermore, with the configuration of the carbon textiles in the carbon TRC specimens presented in Fig. 2d, the working coefficient of textile GC1 in the corresponding TRC composite was also higher than

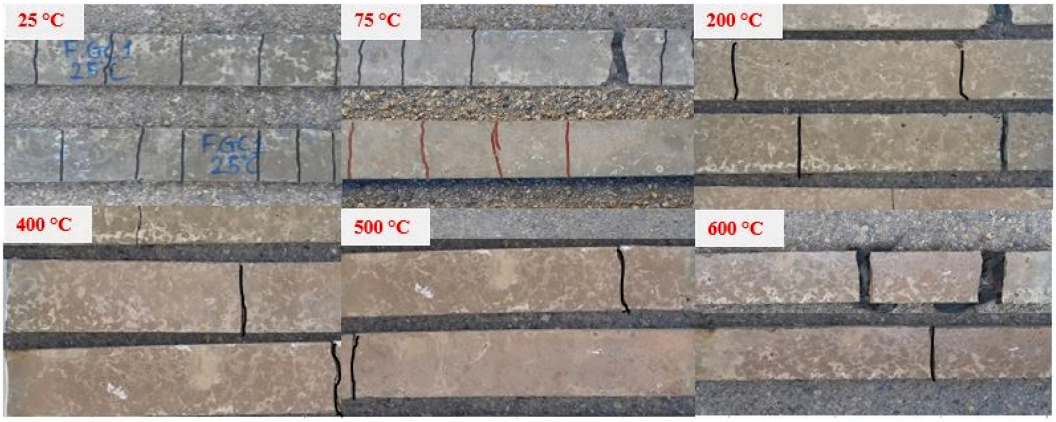

(a) For F.GC1 specimens

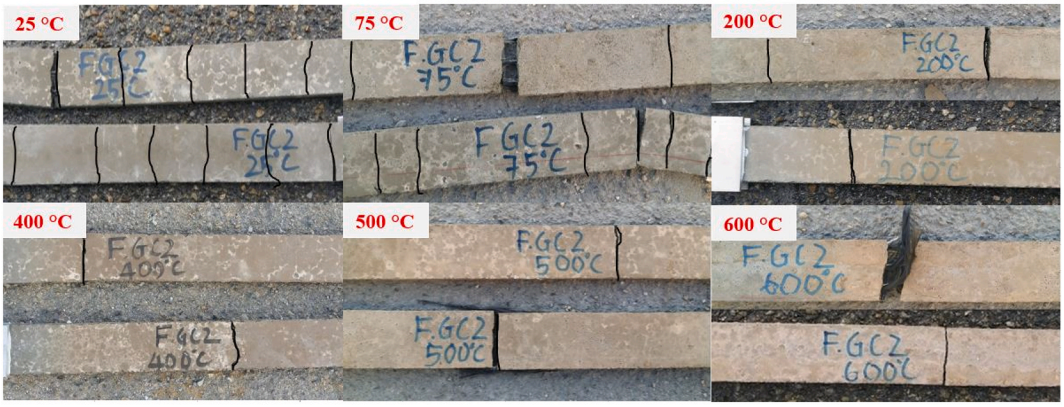

(b) For F.GC2 specimens

Fig. 6. Failure modes of TRC specimens at elevated temperature levels: (a) F.GC1 specimens; (b) F.GC2 specimens.

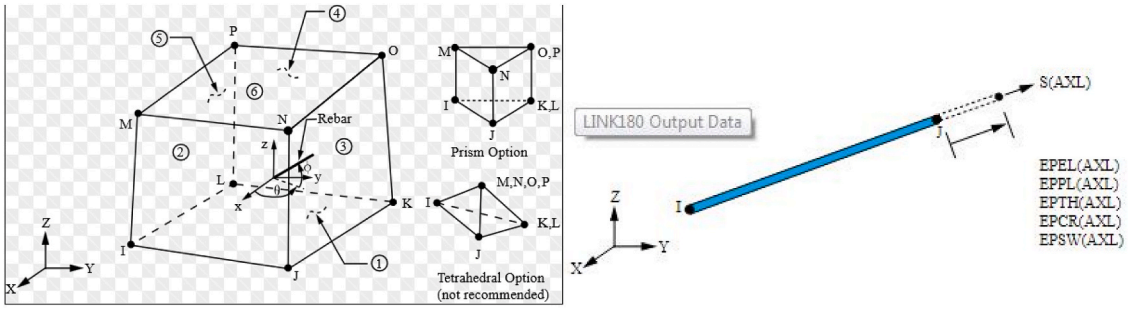

(a) SOLID65 element for concrete matrix. (b) LINK 180 element for carbon textile.

Fig. 7. Element types used in the numerical model [49].

that of specimen F.GC2. Therefore, carbon textile GC1 provided better reinforcement for the ultimate strength of the TRC composite at almost all the temperature levels, except that of 600 °C.

3.2.2. Effect of carbon textile on textile/matrix interaction

The effect of the carbon textile on the interaction between the reinforcement textile and the cementitious matrix of TRC specimens is linked to the textile/matrix bond at the interface. Under the thermal loading of elevated temperature, the modification of the treatment product strongly influenced the bond strength of the textile/matrix interface, changing the thermomechanical behaviour and mechanical properties in the first and second phases.

Concerning the effect of the reinforcement textile on the cracking stress in the first phase, the ratio of cracking stress between the two carbon TRC composites studied was approximately 1.5 times better for the F.GC2 specimens at all temperature levels. The treatment using an amorphous silica product improved the adherence of the GC2 textile/matrix interface more significantly than that of the GC1 textile/matrix interface, treated by the epoxy resin. The improvement of the interface bond strength of F.GC2 can be attributed to the C-S-H gel generated from the reaction between the amorphous silica treatment and the cementitious hydration product (Ca(OH)2) [45]. This thin layer of C-S-H gel gave very good adhesion between the GC2 carbon textile yarns and the cementitious matrix. In addition, this product is not as sensitive to elevated temperature as epoxy resin which was strongly modified by kinetic transitions with the increase of temperature, such as glass transition Tg (around 70 °C), melting, crystallization, decomposition and oxidation (above 450 °C). Thus, bond strength ensured good interaction

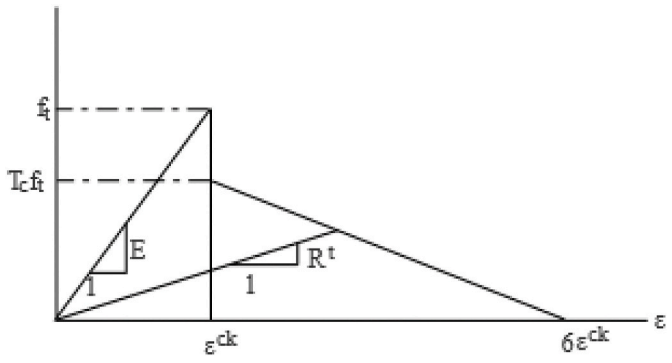

Fig. 8. Stress-strain relationship of the cracked condition (CONCR –Nonlinear Behaviour – Concrete) [48].
Where: f_t = uniaxial tensile cracking stress,
T_c = multiplier for the amount of tensile stress relaxation,
ε^{ck} = uniaxial tensile cracking strain,
R^t = slope (secant modulus) as defined in Fig. 8.

Table 4
Mechanical properties of the component materials of carbon TRC in the numerical model.

Temperature	Carbon textile (LINK 180)			Cementitious matrix (SOLID 65)			
	E_f (GPa)	σ_f (MPa)	η_f	E_m (GPa)	f_t (MPa)	ε_{ck}	Tc
25 °C	143.8	1311.5	0.86	8.41	5.29	6.29×10^{-4}	0.8
75 °C	140.3	1244.7	0.84	6.58	3.76	5.71×10^{-4}	0.8
200 °C	138.6	1152.5	0.66	4.39	3.69	8.41×10^{-4}	0.7
400 °C	107.1	708.8	0.90	3.09	3.28	10.61×10^{-4}	0.6
500 °C	39.7	308.1	0.60	2.29	2.90	12.66×10^{-4}	0.5
600 °C	0	0	–	1.67	2.54	15.21×10^{-4}	0.4

at the textile/matrix interface of the F.GC2 composite for almost all the temperature levels while good textile/matrix interaction was ensured only in the case of low temperature for F.GC1. Moreover, the size of the carbon grid also significantly influenced the load transmission between the reinforcement textile and cementitious matrix. That is why the GC2 carbon textile, with a smaller geometry of 17 mm × 17 mm, gave the best cracking stress value in the first phase for the corresponding TRC composite.

Regarding the elevated temperature effect on the Young's modulus of the first phase, it was observed to have a considerable effect on the epoxy resin treatment, leading to a significant reduction (about 45%) of the Young's modulus of the F.GC1 specimens at temperatures above 75 °C. When the temperature increased to a level that was higher than the glass transition temperature of epoxy resin (Tg about 70 °C), the GC1 textile/matrix interface started to partially debond due to the melting of part of the epoxy resin directly connected to the cementitious matrix. This led to a considerable reduction in the cohesion between the GC1 textile and the cementitious matrix. On the contrary, the F.GC2 specimens presented a progressive decrease in the Young's modulus of the first phase with elevated temperature.

In Fig. 4, the "stress-strain" curves at different temperature levels show the effect of the reinforcement textile on the interaction between the carbon textile and the cementitious matrix in the TRC specimens. The high efficiency of GC2 textile/matrix bond clearly improved the loading capacity of TRC composite in the first and second phases of the "stress-strain" curves of its behaviour. The working capacity of the cementitious matrix greatly benefited from the transfer of tension stress from the reinforcement textile to the cementitious matrix. After the appearance of the first crack, this process occurred along the length of the load transfer and was stopped when the next crack occurred on the surface of TRC specimens [46,47]. Thus, the second phase of the elevated temperature behaviour of the F.GC2 specimens was characterized by drops in stress corresponding to the appearance of cracks. For the F.GC1 specimens, this phase was not clear due to the weakness of the interface bond.

4. Finite element modeling

The finite element method was used for the mesoscale numerical modeling of the elevated temperature behaviour of the TRC composite, in which the material damage of the cementitious matrix could be taken into account by using the cracking model. However, this section presents only the mesoscale modeling for the F.GC2 composites using ANSYS APDL 2015, with the assumption of the perfect bond of the textile/matrix interface [48].

4.1. Numerical model

The modeling procedure includes the choices of the type of elements used, the material model, the mesh, the boundary conditions and loads.

4.1.1. Element types

The type of element chosen for the reinforcement textiles (carbon textile) in this numerical study was LINK180 (3-D Spar or Truss). This element is a 3D spar that can be used to model trusses, sagging cables,

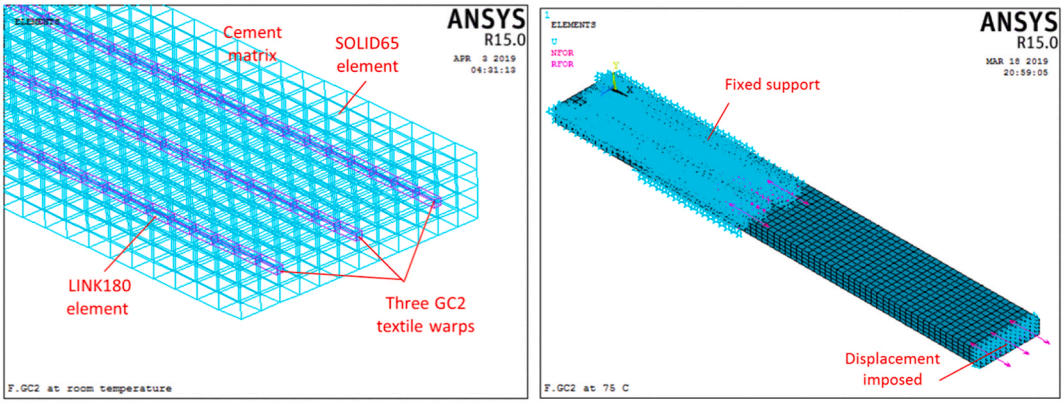

(a) Elements and meshing. (b) Boundary conditions and loads.

Fig. 9. Configuration of meshing, boundary conditions and loads for the F.GC2 specimen model.

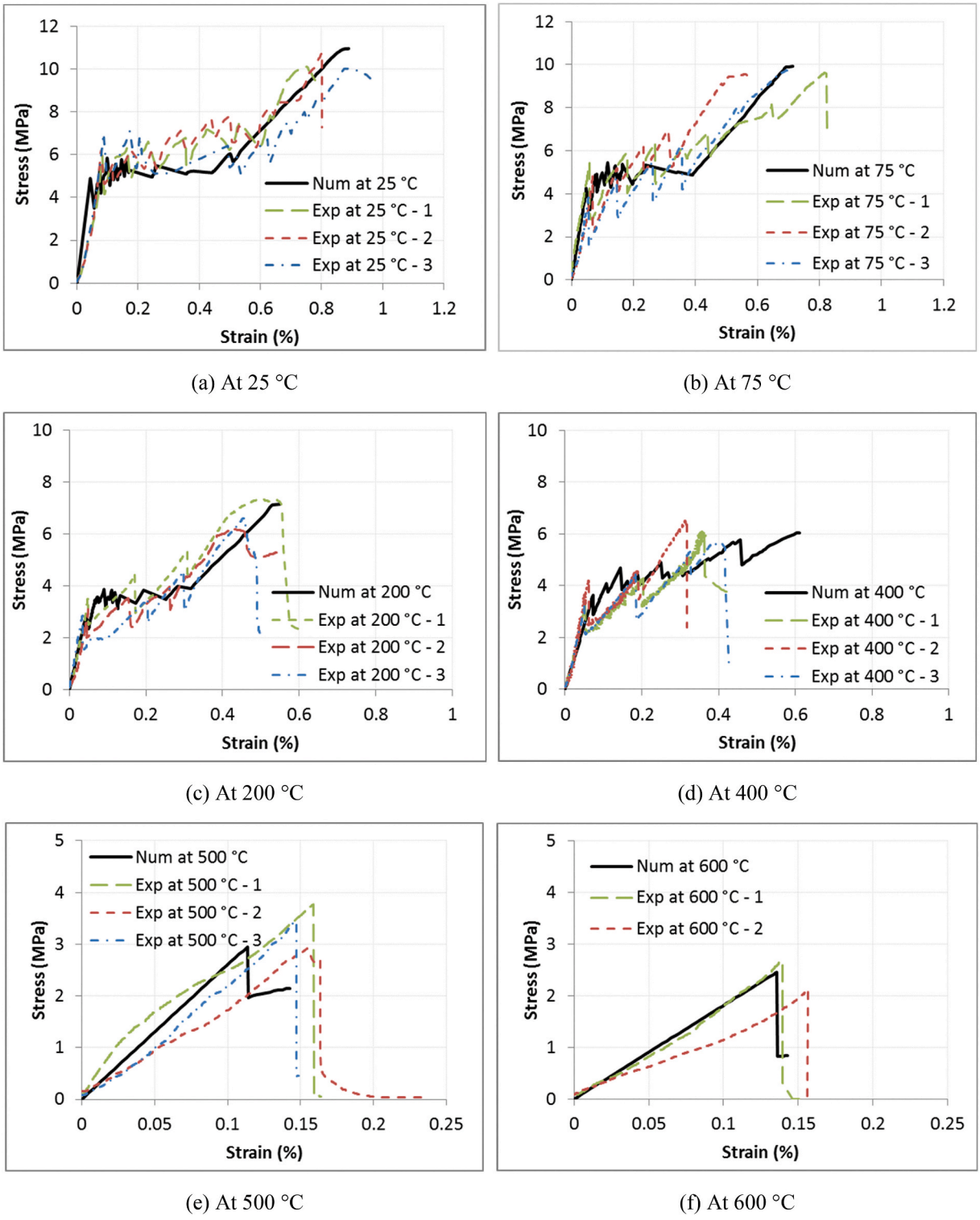

Fig. 10. Numerical results of carbon TRC's behaviour at the temperature from 25 °C to 600 °C.

links, springs, etc. It is a uniaxial element of tension (or compression) with three degrees of freedom at each node: translations in the nodal directions x, y and z (see Fig. 7b). Regarding the element type for the concrete matrix, SOLID65 (3D Reinforced Concrete Solid) was chosen in this numerical study. It allows the presence of four different materials in each element. Therefore, it can combine with reinforcement materials such as steel or textiles to generate a composite material (TRC composite in this case). The concrete material is capable of cracking and crushing directional integration in addition to incorporating plastic and creep behaviour. Fig. 7 below shows both elements in the 3D numerical model for the TRC composite.

Concerning the complicated interaction between the reinforcement textiles and the cementitious matrix, the authors assumed perfect bonding between both components. This assumption was based on the observation of the failure modes of the F.GC2 composite specimens after tensile tests. The experiments showed that the slip between the textile and the matrix at the interface was negligible. This result was obtained from the textile treatment (amorphous silica for carbon textile) to

Table 5
Comparison between the numerical and experimental results of the mechanical properties of F.GC2 at different temperatures.

Temperature	Results	First crack values		Post crack values		
		$\sigma_{T,I}$ (MPa)	$E_{T,I}$ (GPa)	$\sigma_{T,UTS}$ (MPa)	$\varepsilon_{T,UTS}$ (%)	$E_{T,III}$ (GPa)
25 °C	Numerical results	5.31	11.29	10.95	0.889	1.43
	Experimental results	6.38	11.33	10.30	0.813	2.50
75 °C	Numerical results	4.25	8.82	9.92	0.714	1.67
	Experimental results	4.71	9.03	9.64	0.694	1.76
200 °C	Numerical results	3.58	6.66	7.11	0.529	1.48
	Experimental results	3.79	8.48	6.95	0.497	2.13
400 °C	Numerical results	3.64	5.08	6.18	0.722	0.46
	Experimental results	3.63	7.13	6.11	0.359	1.15
500 °C	Numerical results	2.95	2.61			
	Experimental results	3.39	3.75			
600 °C	Numerical results	2.45	1.82			
	Experimental results	2.40	2.14			

improve bond strength and from the contribution of the transversal yarns of the textile (the wefts) against textile/matrix slipping.

4.1.2. Material models

This numerical model was based on the material models for the TRC components in which the material properties were specified for numerical calculation at different temperatures. Concerning the material model for the cementitious matrix, the concrete model (CONCR - Nonlinear Behaviour - Concrete) [48] was chosen in this modeling investigation. It can present the failure mode of fragile materials (concrete, stone, ceramics, etc.) in which cracking and crushing failure are taken into account. The presence of a crack at an integration point is represented through the modification of stress-strain relations by introducing a plane of weakness in a direction normal to the crack face. The stress-strain relationship of the cementitious matrix (cracked in one direction only in the case of TRC composite) is presented in Fig. 8 below.

Regarding the material model for carbon textile, the perfect linear elastic model was chosen to simulate its work under tensile loading. The important parameters of this material model are ultimate strength and Young's modulus. However, in order to take into account the cohesion between three GC2 textile yarns in the TRC composite, an efficiency coefficient (η_f) of the carbon textile used in the carbon TRC (F.GC2) for different temperatures was used in the numerical model (see Table 4). It was calculated by the ratio between the ultimate force of F.GC2 and that of carbon textile GC2 from the experimental results for different temperatures. Its value was calculated for the F.GC2 composite and presented in the author's previous research [31]. As calculated, the efficiency coefficient (η_f) decreased from 0.86 to 0.6 with increasing temperature, except in the case of 400 °C. Table 4 below presents all the calculated parameters of the GC2 carbon textile and cementitious matrix for 6 temperature levels varying from 25 °C to 600 °C. In Table 4, E_f, σ_f are the ultimate strength and Young's modulus of the carbon textile, η_f is the efficiency coefficient of the carbon textile used in the carbon TRC (F.GC2) at different temperatures, E_m and f_t are the ultimate strength and initial stiffness of the cementitious matrix, ε_{ck} and Tc are the uniaxial tensile cracking strain and the multiplier for the amount of tensile stress relaxation defined by the concrete model (CONCR - Nonlinear Behaviour - Concrete).

4.1.3. Meshing, boundary conditions and loads

The numerical model was constructed step by step with Ansys APDL 2015. Firstly, a block of the cementitious matrix corresponding to half of the corresponding dimension of the TRC specimen (used in the experimental test) was created (11.5 mm × 51 mm x 370 mm). Then, three longitudinal textile yarns were also created in their position as in the real F.GC2 specimen. This model was meshed in parallelepiped form for the SOLID65 elements and a reinforced truss bar for the LINK180 elements. The size of the elements depended on the size of each edge of the model and the average value of the size was about 4 mm (see Fig. 9a). Concerning the boundary conditions and loads of the numerical model, they were configured like those of an experimental test. In reality, two ends of the TRC specimens were bonded with the aluminium plates to transfer the tensile force. The length of the bonding part was 160 mm for each end. Thus, all the nodes of this bonding part of the first end were positioned on fixed supports with all movements blocked according to three coordinated axes. The mechanical load was applied to the other end of the TRC specimen by the imposed displacement. The speed of the applied load was modified over time by loading steps and sub-steps. Fig. 9b shows the boundary condition and loading configuration for the numerical model.

4.2. Numerical results

This section presents the results obtained from the numerical model for the F.GC2 composite at different temperatures from 25 °C to 600 °C, including the elevated temperature behaviour, the development of cracking, and failure mode of the TRC specimen.

4.2.1. Global behaviour of the carbon TRC composite at elevated temperatures

Fig. 10 presents the numerical results of the elevated temperature behaviour of the F.GC2 composite in comparison with those of the experiment. According to the numerical results, at moderate temperatures (from 25 °C to 200 °C) the carbon TRC presented a strain hardening behaviour with three distinguishable phases (see Fig. 10a,b,c). The first phase is linear, and its stiffness (E_1) is closely followed by the mixing law of the composite material while the cracking stress (σ_I) greatly depends on the matrix strength. The second phase is characterized by several drops in stress which correspond with the appearances of cracks on the specimen. However, these drops in stress are smaller than those observed in the experiment. The third phase is almost linear until the limit state of the textile yarns because the cracking occurred completely within the cementitious matrix, and only the reinforcement textile was subjected to work (see Fig. 10 a,b,c).

As can be seen for the numerical result at 400 °C (see Fig. 10d), the strength of the three yarns of the GC2 textile is just a little higher than that of the concrete matrix. Therefore, a strain hardening behaviour with two phases is drawn for the F.GC2 specimen, as presented in Fig. 10d. Both phases of this behaviour are also described as similar to the cases of moderate temperatures. At temperature levels equal to or higher than 500 °C, the carbon TRC presents a brittle behaviour like that of the concrete matrix (Fig. 10e and f). It breaks after the first drop in stress, corresponding to the only crack on the specimen surface.

In comparison with the experimental results, the numerical model shows good agreement, in particular in the first and third phases of the carbon TRC's behaviour at different temperatures. In the cracking phase, the complex work between the reinforcement textile and concrete matrix in the experiment actually caused a slight difference between both the experimental and numerical results. The numerical model could not take into account the complex experimental phenomena that occurred in the cracking phase, such as the slip between textile filaments, the dynamic effect and the local increase in elongation of the specimen after a drop in force. Table 5 below presents the comparison of the mechanical properties of the carbon TRC between both the experimental and numerical results at elevated temperatures.

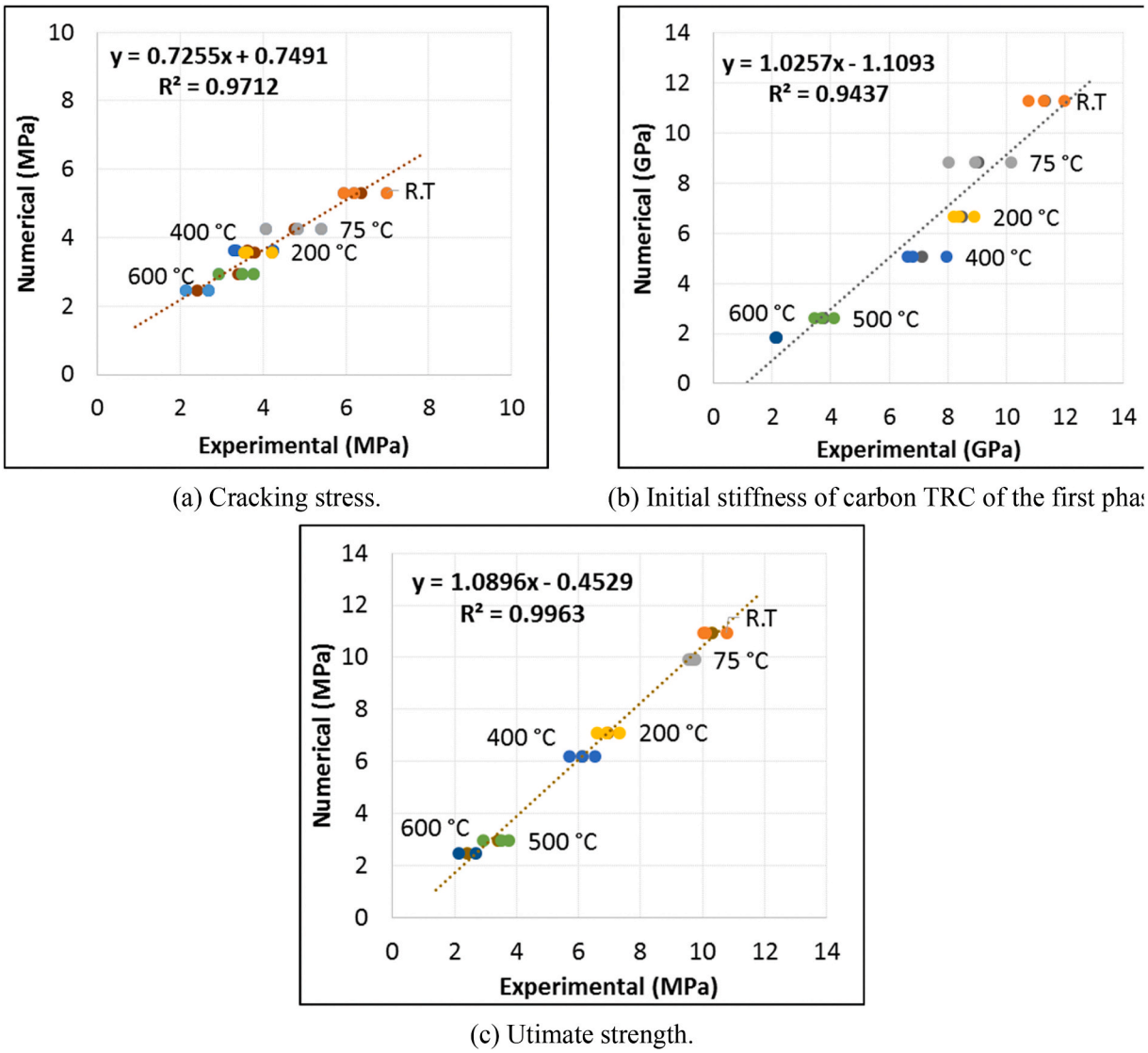

Fig. 11. Experimental results versus numerical modeling results at different temperatures: (a) cracking stress; (b) Initial stiffness of carbon TRC of the first phase; (c) ultimate strength.

Fig. 11 shows the comparison of mechanical properties at different temperatures between the experimental and numerical results using the computational tools proposed. Fig. 11 shows that the coefficients of determination are good values for all cases of this comparison: R^2 = 0.97, 0.94 and 0.99 for cracking stress, the initial stiffness of carbon TRC of the first phase, and ultimate strength, respectively. Therefore, it can be said that the numerical model provides a fairly good prediction of the mechanical properties of the composite TRC at elevated temperatures. This means that the working together of the carbon textile and cementitious matrix in the TRC composite was reasonably reflected. However, in the case of ultimate deformation at 400 °C, there was a significant difference between the experimental and numerical results that could be explained by the complex work in the cracking phase.

4.2.2. *Local behaviour of TRC components*

4.2.2.1. Cementitious matrix. In general, the cementitious matrix presents a brittle behaviour in the TRC composite, as shown in its material model. However, its behaviour depended slightly on the position of the nodes studied. With three nodes studied, as shown in Fig. 12a, the cementitious matrix gave different curves of its behaviour in the post-peak phase (see Fig. 12b). These relationships depend entirely on the order in which the cracks appear on the cross-sections related to these nodes. The numerical model allowed observing the development of a crack on a cross-section of the TRC specimen. With three carbon textile warps as reinforcement, the cementitious matrix elements around a warp were in a more likely condition to crack, and cracking occurred at these elements first. Then, the micro-crack gradually developed towards the elements in the same cross-section because the element cracking reduced the efficiency of the cross-section to support the tensile force (see Fig. 12c). Finally, this process stopped when the cementitious matrix in this cross-section was completely cracked, and therefore there was a drop in the tensile stress on the "stress-strain" curve. The cracking of the cementitious matrix would be continued with another cross-section if the warps of the carbon textile still ensured the load-bearing capacity, as in the cases of moderate temperatures (from 25 °C to 400 °C). Otherwise, the TRC specimen was immediately broken after the appearance of the first crack, as in the case of the temperature higher 500 °C.

Concerning the position of the cross-section where the first crack occurred, it was always the cross-section next to the fixed support zone (see Fig. 12c). This result was in good agreement with the observation of the failure modes of the TRC specimens in the experiment. This could be explained by the effect of dynamic phenomena as well as that of the

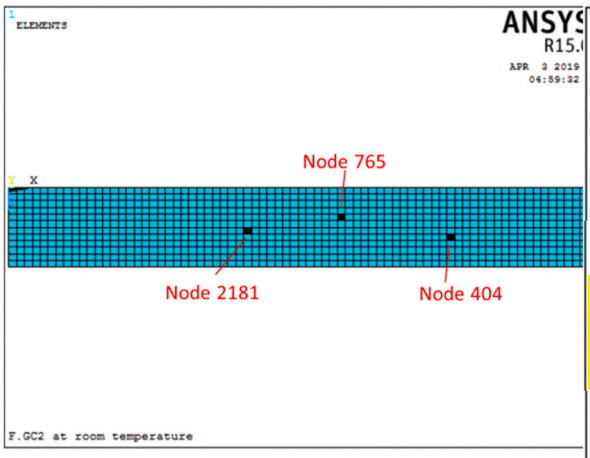

(a) Position of the nodes studied.

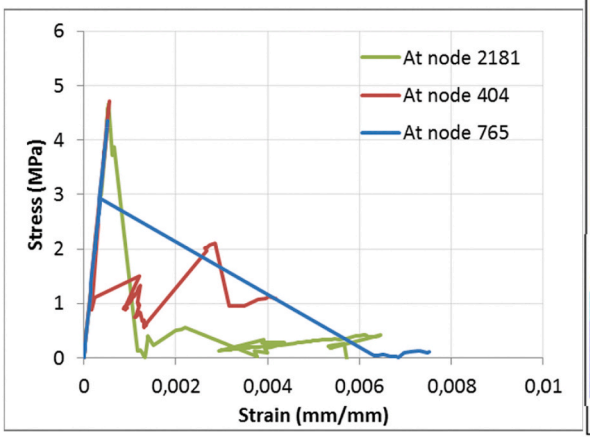

(b) Fragile behaviour of the matrix at the nodes studied.

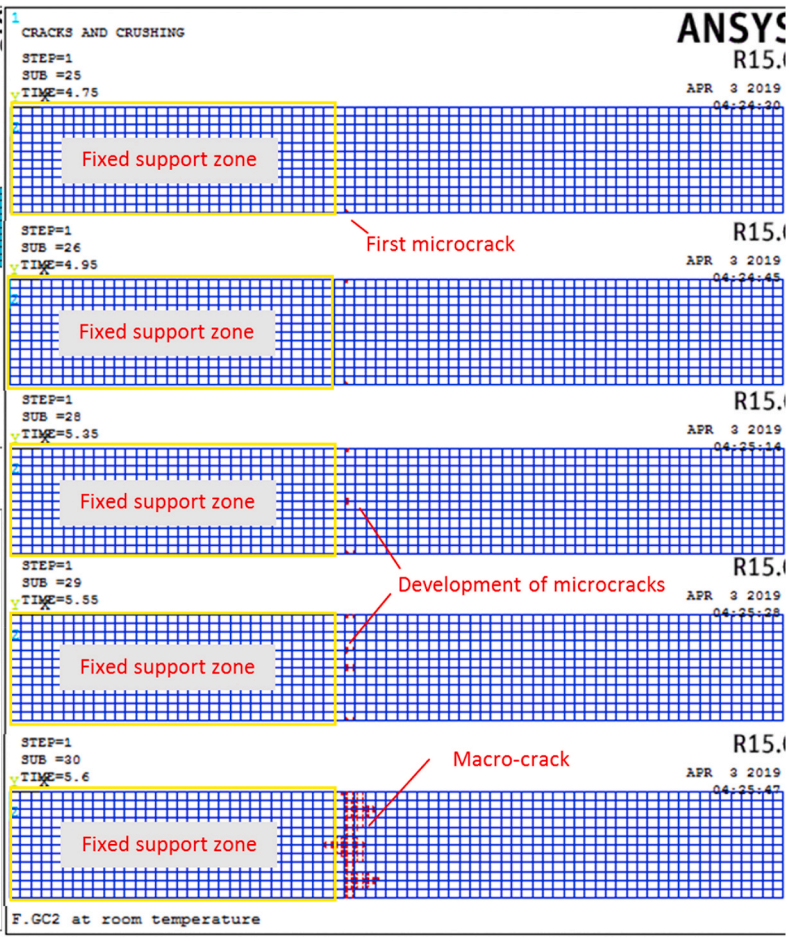

(c) Development of the first crack on a cross section of the TRC specimen; room temperature: 25 °C.

Fig. 12. Local behaviour of the cementitious matrix in the numerical model (in the case at 25 °C).

concentration in stress when the specimen was subjected to tensile force. In the experiment, the first end of the TRC specimen was bonded with the aluminium plates (as a reinforcement with 160 mm in length) to transfer the tensile force from the traverse of the machine to the specimen. The fixed support zone in the numerical model was built with the boundary condition as this bonding part. Thus, when tensile force was applied to the TRC specimen by the imposed displacement, the cross-section next to the fixed support zone became the most dangerous one because of the stress concentration phenomenon. Furthermore, all the nodes in the fixed support zone were blocked against any movement according to three coordinated axes, while the rest was moved in the direction of the imposed displacement. This led to the effect of the dynamic phenomena on the cross-section next to the fixed support zone. That is why the crack occurred in this position first.

4.2.2.2. Reinforcement textile. In the numerical model, the carbon textile always exhibted linear behaviour until its failure. However, when cracking occurred in the cementitious matrix, the redistribution of the internal force occurred in three textile warps. After the appearance of the first crack, the stress of the carbon textile warps increased abruptly because they had to supported in addition the part of the internal force from the cementitious matrix that had just completely cracked in the same section. For example, in the case at room temperature, a stress jump of about 298 MPa (from 120 MPa to 418 MPa) could be observed on the carbon textile warps (see Fig. 13a and b) when the first crack occurred in the cementitious matrix.

After the first crack, the cementitious matrix progressively cracked until complete cracking, while the stress of the textile warps increased gradually but with a small tendency corresponding with the cracking phase of the TRC behaviour (see Fig. 13b and c). In the third phase, the stress of the three warps on all the cross-sections was similar. The numerical tests were stopped when the carbon warps reached the limit state of their deformation. Fig. 13d shows the distribution in tensile stress in three GC2 warps at the last step of the modeling calculation.

4.2.3. Failure mode

The numerical calculations showed a single mode of brittle fracture on the F.GC2 specimen at different temperatures. However, this failure mode could be divided into two modes depending on the elevated temperature level. At the temperature levels ranging from 25 °C to 400 °C, the cementitious matrices of the F.GC2 specimens were completely cracked before being broken by the damage of the textile warps. The cracking zone was widened gradually on the surface of the TRC specimen, as shown in Fig. 14a. Otherwise, at the temperature levels higher 500 °C, only one crack was observed after the numerical test. This is consistent with the observation of the failure mode for the specimens of the experiment at the same temperature. Table 6 below compares the failure modes between the experimental and numerical results in two ranges of elevated temperature levels: from 25 °C to 400 °C and from 500 °C to 600 °C.

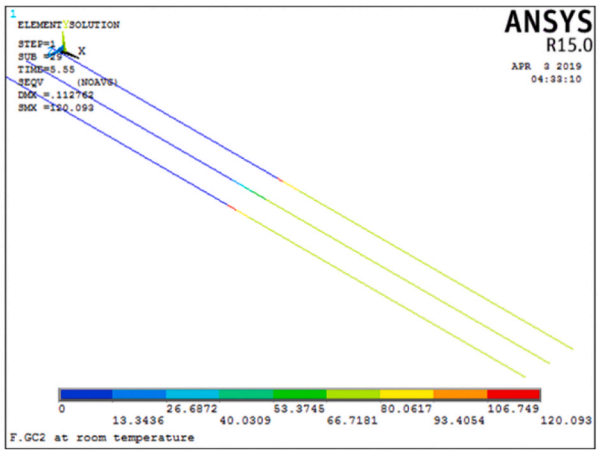

(a) Stress evolution jump in reinforcement at the step before the first crack of the cementitious matrix (stress in MPa)

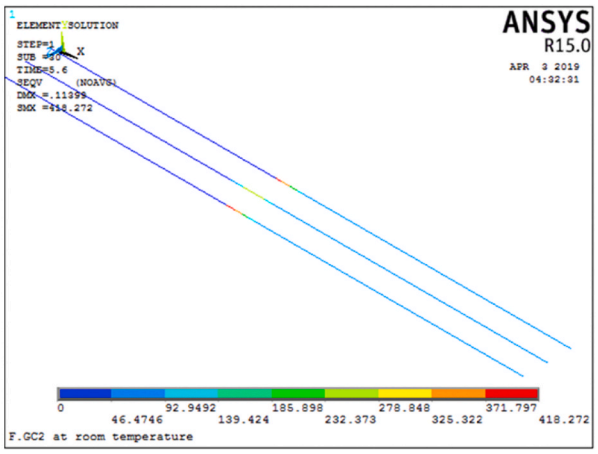

(b) Stress evolution jump in reinforcement at the next step (stress in MPa)

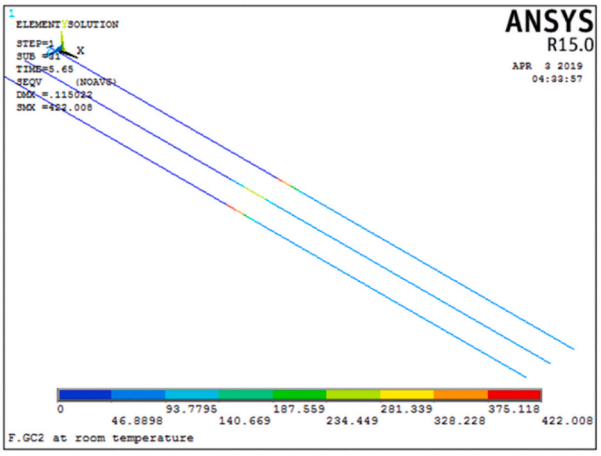

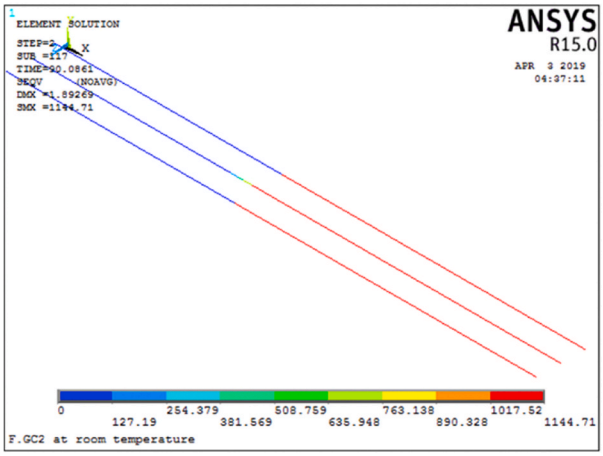

Fig. 13. Stress evolution within carbon warps before and after the appearance of the first crack (stress in MPa); room temperature: 25 °C.

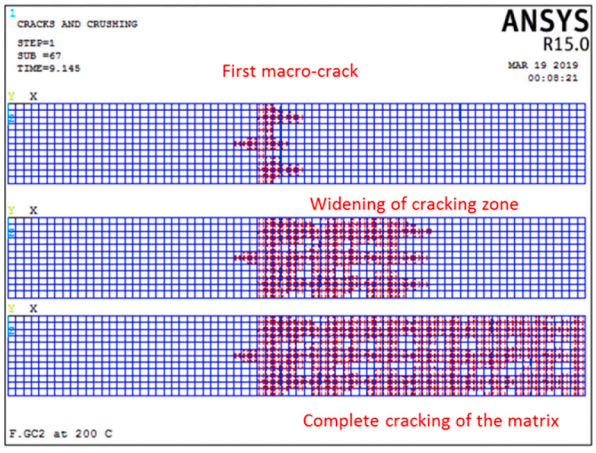

(a) Crack development for ~~the~~ temperatures from 25 °C to 400 °C.

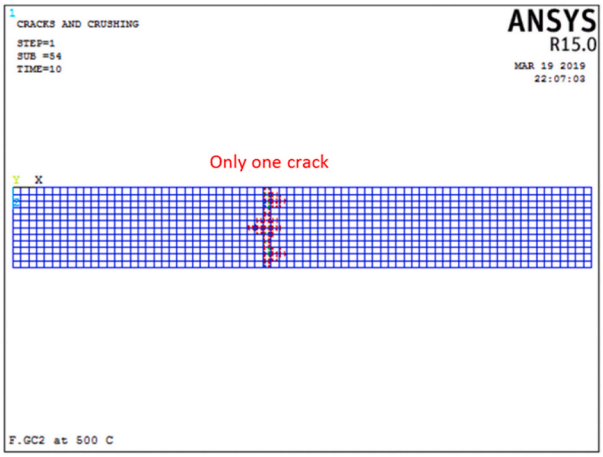

(b) Only one crack for the specimen at the temperature above 500 °C.

Fig. 14. Failure mode of carbon TRC specimens at different temperatures.

5. Conclusions and future work

This paper presented and analyzed experimental and numerical modeling results at the mesoscale concerning the elevated temperature behaviour of carbon TRC composites. In this study, two carbon textiles with different geometries and treatment products were used to reinforce

Table 6
Comparison of the rupture modes between the experimental and numerical results.

Temperature	Experimental results	Numerical results
From 25 °C to 400 °C		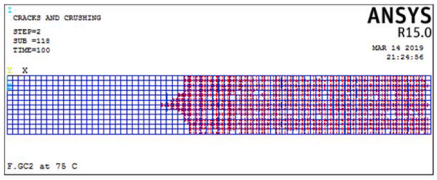
From 500 °C to 600 °C		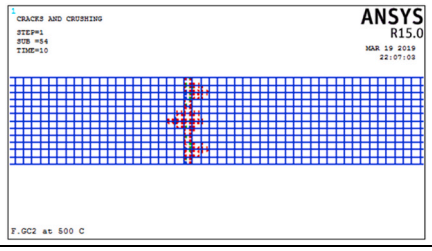

a refractory concrete matrix. Both carbon TRC specimens were tested under simultaneous mechanical loading and elevated temperature levels ranging from 25 °C to 600 °C. Regarding the numerical approach, a numerical model was developed using the finite element method on ANSYS APDL software. This model took into account the material damage of the cementitious matrix by using the nonlinear concrete behaviour model (CONCR) for crack modeling while perfect bonding was assumed for the textile yarns and the cementitious matrix interface in the numerical calculations. From the experimental and numerical results obtained, the following conclusions can be drawn:

- Both carbon TRC specimens provided a strain-hardening behaviour with two or three distinguishable phases at moderate temperature and brittle behaviour at an elevated temperature, depending on the carbon textile reinforcement. A good bond between the matrix and reinforcement is essential to achieve such behaviour. The mesh spacing (and thus reinforcement ratio) can, however, lead to differences in the crack development observed. The GC1 textile always ensured better reinforcement in the ultimate strength of the TRC composite at elevated temperature thanks to the complete impregnation of the textile yarns in the epoxy resin product used, but it also presented a negative temperature effect on the textile/matrix interface bond. On the contrary, the GC2 textile gave good textile/matrix interface bond strength thanks to the treatment of the textile with amorphous silica. This improved the interaction between both TRC components in the first and second phases of the carbon TRC's behaviour at different temperatures.
- The mesoscale numerical modeling for the F.GC2 composite was able to predict its global behaviour numerically with three phases at temperature levels lower than 400 °C and splitting behaviour at an elevated temperature. This elevated temperature behaviour of the F.GC2 composite greatly depended on the correlation of the strength of its components (GC2 textile and cementitious matrix). The numerical model could also represent the cracking phase with drops in stress, corresponding to multi-cracks of the cementitious matrix in failure mode. In comparison with the experimental results, interesting agreement was obtained between the "stress-strain" curves of both the experimental and numerical results at different temperatures.
- The numerical specimens exhibited failure modes with transversal cracks on their surfaces in the cases of elevated temperature levels lower than 400 °C, and with only one crack for higher temperature levels. This result is in good agreement with the observation of failure modes in the experiment. The numerical model also presented the progressive development of a crack on one transversal cross-section of the TRC specimen, from a micro-crack to a complete crack.
- The assumption of a perfect bond for the textile – matrix interface resulted in a slight difference in tensile behaviour and failure mode between the numerical and experimental results of the F.GC2 composite. During the experiment, several phenomena occurred during the thermomechanical tests, such as the slip between the filament groups of the reinforcement textile, and the dynamic effect after cracking, which led to the very fast rise in the strain of the TRC specimens.

For future works, it will be necessary to carry out a parametric study to investigate several factors that could not be explored experimentally, such as the effect of the reinforcement ratio and the influence of the measurement zone. It would also be interesting to add the thermal properties of material components to develop a numerical model of the thermomechanical regime at constant force. Such a finite element model could be used to predict the rupture temperature and maximum exposure duration of TRC composites in the case of fire.

Declaration of competing interest

The authors declare that they have no known competing financial interests or personal relationships that could have appeared to influence the work reported in this paper.

Acknowledgments

This research was performed with the financial support of LMC2 (thanks to its industrial projects) for the experimental works, and with the financial support of a doctoral scholarship from the Ministry of Education and Training (Vietnam) for the first author. We would like to thank Kerneos Aluminate Technologies, France for supplying the materials (cement, aggregates, super-plasticizer). We would also like to thank the technicians (Mr. E. JANIN, Mr. N. COTTET) from the Civil Engineering department of IUT Lyon 1 and LMC2, University of Lyon 1 for their technical support.

Appendix A. Supplementary data

Supplementary data to this article can be found online at https://doi.org/10.1016/j.firesaf.2020.103186.

References

[1] M. Butler, M. Lieboldt, V. Mechtcherine, Application of textile-reinforced concrete (TRC) for structural strengthening and in prefabrication. Proceedings of the

International Conference on Advanced Concrete Materials (ACM), Stellenbosch, South Africa, 2010, pp. 125–134.
[2] V. Mechtcherine, Novel cement-based composites for the strengthening and repair of concrete structures, Construct. Build. Mater. 41 (Apr. 2013) 365–373.
[3] Q.T. Shubhra, A. Alam, M. Quaiyyum, Mechanical properties of polypropylene composites: a review, J. Thermoplast. Compos. Mater. 26 (3) (Apr. 2013) 362–391.
[4] B. Mobasher, V. Dey, Z. Cohen, A. Peled, Correlation of constitutive response of hybrid textile reinforced concrete from tensile and flexural tests, Cement Concr. Compos. 53 (Oct. 2014) 148–161.
[5] R. Contamine, A. Si Larbi, P. Hamelin, Contribution to direct tensile testing of textile reinforced concrete (TRC) composites, Mater. Sci. Eng., A 528 (29) (Nov. 2011) 8589–8598.
[6] C. Soranakom, B. Mobasher, Correlation of tensile and flexural responses of strain softening and strain hardening cement composites, Cement Concr. Compos. 30 (6) (Jul. 2008) 465–477.
[7] Yunxing Du, Mengmeng Zhang, Fen Zhou, Deju Zhu, Experimental study on basalt textile reinforced concrete under uniaxial tensile loading, Construct. Build. Mater. 138 (May 2017) 88–100.
[8] R. Contamine, Contribution à l'étude du comportement mécanique de composites textile-mortier : application à la réparation et/ou renforcement de poutres en béton armé vis-à-vis de l'effort tranchant, Ph.D. thesis dissertation, Université Claude Bernard - Lyon I, 2011 ([in French]).
[9] B.T. Truong, Formulation, performances mécaniques, et applications, d'un matériau TRC pour le renforcement et la réparation de structures en béton/et béton armé: Approches expérimentale et numérique, Ph.D. thesis dissertation, Université de Lyon, 2016 ([in French]).
[10] T. Tlaiji, Développement et caractérisation du comportement thermomécanique des matériaux composites TRC, Ph.D. thesis dissertation, Université de Lyon, 2018 ([in French]).
[11] M. Ezziane, T. Kadri, L. Molez, R. Jauberthie, A. Belhacen, High temperature behaviour of polypropylene fibres reinforced mortars, Fire Saf. J. 71 (2015) 324–331.
[12] D. Gao, D. Yan, X. Li, Splitting strength of GGBFS concrete incorporating with steel fiber and polypropylene fiber after exposure to elevated temperatures, Fire Saf. J. 54 (2012) 67–73.
[13] O. Arioz, Effects of elevated temperatures on properties of concrete, Fire Saf. J. 42 (2007) 516–522.
[14] M. Husem, The effects of high temperature on compressive and flexural strengths of ordinary and high-performance concrete, Fire Saf. J. 41 (2006) 155–163.
[15] D.A.S. Rambo, F. de Andrade Silva, R.D. Toledo Filho, O. da Fonseca Martins Gomes, Effect of elevated temperatures on the mechanical behavior of basalt textile reinforced refractory concrete", Mater. Des. 65 (1980-2015) 24–33. Jan. 2015.
[16] T.H. Nguyen, Contribution à l'étude du comportement thermomécanique à très haute température des matériaux composites pour la réparation et/ou le renforcement des structures de Génie Civil, Ph.D. thesis dissertation, Université Claude Bernard - Lyon I, 2015 ([in French]).
[17] F. de A. Silva, M. Butler, S. Hempel, R.D. Toledo Filho, V. Mechtcherine, Effects of elevated temperatures on the interface properties of carbon textile-reinforced concrete, Cement Concr. Compos. 48 (Apr. 2014) 26–34.
[18] D.A.S. Rambo, Y. Yao, F. de Andrade Silva, R.D. Toledo Filho, B. Mobasher, Experimental investigation and modelling of the temperature effects on the tensile behavior of textile reinforced refractory concretes, Cement Concr. Compos. 75 (Jan. 2017) 51–61.
[19] D.A.S. Rambo, F. de Andrade Silva, R.D. Toledo Filho, N. Ukrainczyk, E. Koenders, Tensile strength of a calcium-aluminate cementitious composite reinforced with basalt textile in a high-temperature environment, Cement Concr. Compos. 70 (Jul. 2016) 183–193.
[20] M.T. Tran, X.H. Vu, E. Ferrier, Experimental and analytical analysis of the effect of fibre treatment on the thermomechanical behaviour of continuous carbon textile subjected to simultaneous elevated temperature and uniaxial tensile loadings, Construct. Build. Mater. 183 (Sep. 2018) 32–45.
[21] M.T. Tran, X.H. Vu, E. Ferrier, Treatment effect on failure mode of industrial carbon textile at elevated temperature, in: Handbook of Materials Failure Analysis with Case Studies from the Electronics and Textile Industries, Abdel Makhlouf, Mahmood Aliofkhazraei., Elsevier, 2019.
[22] T. Hulin, D.H. Lauridsen, K. Hodicky, J.W. Schmidt, H. Stang, Influence of basalt FRP mesh reinforcement on high-performance concrete thin plates at high temperatures", J. Compos. Construct. 20 (1) (2015).
[23] H.W. Reinhardt, M. Krüger, M. Raupach, Behavior of textile-reinforced concrete in fire, ACI Spec. Publ. 250 (2008) 99–110.
[24] Z.C. Tetta, Dionysios A. Bournas, TRM vs FRP jacketing in shear strengthening of concrete members subjected to high temperatures, Compos. B Eng. 106 (2016) 190–205.
[25] S.M. Raoof, Dionysios A. Bournas, TRM versus FRP in flexural strengthening of RC beams: behaviour at high temperatures, Construct. Build. Mater. 154 (2017) 424–437.
[26] S.M. Raoof, Dionysios A. Bournas, Bond between TRM versus FRP composites concrete at high temperatures, Compos. B Eng. 127 (2017) 150–165.
[27] I. Colombo, M. Colombo, A. Magri, G. Zani, M. di Prisco, Textile reinforced mortar at high temperatures, Appl. Mech. Mater. 82 (2011) 202–207.
[28] T. Tlaiji, X.H. Vu, E. Ferrier, A. Si Larbi, Thermomechanical behaviour and residual properties of textile reinforced concrete (TRC) subjected to elevated and high temperature loading: experimental and comparative study, Compos. B Eng. 144 (Jul. 2018) 99–110.
[29] S. Xu, L. Shen, J. Wang, The high-temperature resistance performance of TRC thin-plates with different cementitious materials: experimental study, Construct. Build. Mater. 115 (Jul. 2016) 506–519.
[30] O. Homoro, X.H. Vu, E. Ferrier, Experimental and analytical study of the thermo-mechanical behaviour of textile-reinforced concrete (TRC) at elevated temperatures: role of discontinuous short glass fibres, Construct. Build. Mater. 190 (Nov. 2018) 645–663.
[31] M.T. Tran, X.H. Vu, E. Ferrier, Mesoscale experimental investigation of thermomechanical behaviour of the carbon textile reinforced refractory concrete under simultaneous mechanical loading and elevated temperature, Construct. Build. Mater. 217 (Aug. 2019) 156–171.
[32] D. Ehlig, F. Jesse, M. Curbach, High temperature tests on textile reinforced concrete (TRC) strain specimens, in: Presented at the International RILEM Conference on Material Science - MATSCI, Aachen University, 2010, pp. 141–151.
[33] T.H. Nguyen, X.H. Vu, A. Si Larbi, E. Ferrier, Experimental study of the effect of simultaneous mechanical and high-temperature loadings on the behaviour of textile-reinforced concrete (TRC), Construct. Build. Mater. 125 (Oct. 2016) 253–270.
[34] M. Saidi, X.H. Vu, E. Ferrier, Experimental and analytial analysis of the thermomechanical behaviour at elevated temperature of the textile reinforced concrete (TRC) Effet of the hydric state, in: Presented at the 9th International Conference on Fibre-Reinforced Polymer (FRP) Composites in Civil Engineering, Paris, 2018, pp. 844–852.
[35] N.W. Portal, K. Lundgren, A.M. Walter, J.O. Frederiksen, L.N. Thrane, Numerical modelling of textile reinforced concrete, in: Presented at the the VIIIth International Conference on Fracture Mechanics of Concrete and Concrete Structures, Toledo, 2013.
[36] N.W. Portal, L.N. Thrane, K. Lundgren, Flexural behaviour of textile reinforced concrete composites: experimental and numerical evaluation, Mater. Struct. 50 (1) (Aug. 2016) 4.
[37] M. El Kadi, T. Tysmans, S. Verbruggen, J. Vervloet, M. De Munck, J. Wastiels, D. Van Hemelrijck, A layered-wise, composite modelling approach for fibre textile reinforced cementitious composites, Cement Concr. Compos. 94 (Nov. 2018) 107–115.
[38] P. Larrinaga, C. Chastre, J.T. San-José, L. Garmendia, Non-linear analytical model of composites based on basalt textile reinforced mortar under uniaxial tension, Compos. B Eng. 55 (Dec. 2013) 518–527.
[39] P. Larrinaga, C. Chastre, H.C. Biscaia, J.T. San-José, Experimental and numerical modeling of basalt textile reinforced mortar behavior under uniaxial tensile stress, Mater. Des. 55 (Mar. 2014) 66–74.
[40] E. Bertolesi, F.G. Carozzi, G. Milani, C. Poggi, Numerical modeling of fabric reinforce cementitious matrix composites (FRCM) in tension, Construct. Build. Mater. 70 (Nov. 2014) 531–548.
[41] J. Blom, J. Wastiels, Modeling textile reinforced cementitious composites-Effect of elevated temperatures, in: Presented at the the 19th International Conference on Composite Materials, 2013.
[42] Z.I. Djamai, M. Bahrar, F. Salvatore, A. Si Larbi, M. El Mankibi, Textile reinforced concrete multiscale mechanical modelling: application to TRC sandwich panels, Finite Elem. Anal. Des. 135 (Nov. 2017) 22–35.
[43] P.L. Nguyen, X.H. Vu, E. Ferrier, Characterization of pultruded carbon fibre reinforced polymer (P-CFRP) under two elevated temperature-mechanical load cases: residual and thermo-mechanical regimes, Construct. Build. Mater. 165 (Mar. 2018) 395–412.
[44] P.L. Nguyen, X.H. Vu, E. Ferrier, Elevated temperature behaviour of carbon fibre-reinforced polymer applied by hand lay-up (M-CFRP) under simultaneous thermal and mechanical loadings: experimental and analytical investigation, Fire Saf. J. 100 (Sep. 2018) 103–117.
[45] M. Lu, H. Xiao, M. Liu, X. Li, H. Li, L. Sun, Improved interfacial strength of SiO2 coated carbon fiber in cement matrix, Cement Concr. Compos. 91 (Aug. 2018) 21–28.
[46] M. Saidi, A. Gabor, Use of distributed optical fibre as a strain sensor in textile reinforced cementitious matrix composites, Measurement 140 (Jul. 2019) 323–333.
[47] M. Saidi, A. Gabor, Experimental analysis of the tensile behaviour of textile reinforced cementitious matrix composites using distributed fibre optic sensing (DFOS) technology, Construct. Build. Mater. 230 (Jan. 2020) 117–127.
[48] ANSYS, in: P. Kohnke (Ed.), Theory Reference for the Echanical APDL and Mechanical Applications, ANSYS Inc, 2009.
[49] ANSYS, Mechanical APDL Element Reference", vol. 14, ANSYS Inc, Release, 2011.